

# Mechanical and fracture behavior of polypropylene/poly(ethylene-co-vinyl alcohol) blends compatibilized with ionomer Na<sup>+</sup>

M. Montoya<sup>a</sup>, M.J. Abad<sup>a</sup>, L. Barral<sup>a,\*</sup>, C. Bernal<sup>b</sup>

<sup>a</sup> Grupo de Polímeros, Departamento de Física, E.U.P.-Ferrol, Universidad de A Coruña, Avda. 19 febrero, s/n. 15405 Ferrol, Spain

<sup>b</sup> Instituto de Investigaciones en Ciencia y Tecnología de Materiales (INTEMA), Universidad Nacional de Mar del Plata, Argentina, Juan B. Justo 4302 (B7608FDQ) Mar del Plata, Argentina

Received 10 June 2005; received in revised form 28 July 2005; accepted 3 August 2005

Available online 19 September 2005

## Abstract

In this work the deformation and fracture behavior of PP/EVOH blends compatibilized with ionomer Na<sup>+</sup> at room and low temperature was studied. Uniaxial tensile tests on dumb-bell samples and fracture tests on single-edge notched bending (SENB) specimens were performed for 10 wt.% and 20 wt.% EVOH blends with different ionomer content at 23 °C and –20 °C. The incorporation of EVOH to PP led to less ductile materials in tension as judged by the lower values of the ultimate tensile strain displayed by all PP/EVOH blends in comparison to neat PP. In contrast, the ionomer Na<sup>+</sup> addition partially counteracted this effect. The compatibilizing effect of ionomer Na<sup>+</sup> was also evident in fracture results since higher values of the fracture parameter were obtained for the ternary blends. SEM observations also confirmed this effect. On the other hand, PP/EVOH blends exhibited different fracture behavior with test temperature. All blends showed “pseudo stable” behavior at room temperature characterized by apparently stable crack growth that could not be externally controlled. On the contrary, blends behaved as semi-brittle at –20 °C with some amount of stable crack growth preceding unstable brittle fracture. Finally, irrespectively of the temperature or the ionomer content all PP/EVOH blends exhibited more ductile fracture behavior with a higher tendency to stable crack propagation than neat polypropylene.

© 2005 Elsevier Ltd. All rights reserved.

**Keywords:** Mechanical properties; Fracture behavior; Polypropylene; EVOH; PP/EVOH blends

## 1. Introduction

Polymer blends are an important route for the development of new polymeric materials. In these blends, the

components are combined to improve certain properties as well as to minimize the cost/property ratio. Obtaining a low-cost material for packaging and hydrocarbons transport, is still a difficult problem to be solved as barrier as well as mechanical properties are simultaneously required. Facility to process at low cost, recyclability and optical clarity (specially for food packaging) are also needed. A common used practice in industry is to

\* Corresponding author. Fax: +349 81 337401.  
E-mail address: [labpolim@udc.es](mailto:labpolim@udc.es) (L. Barral).

blend a small quantity of a barrier material into a low-cost material to obtain a low-cost product with improved barrier properties.

The polypropylene (PP)/poly(ethylene-co-vinyl alcohol) (EVOH) blends are a good example. Both polymers are useful as packaging materials [1]. In addition, EVOH has excellent barrier properties to gases and hydrocarbons and a good chemical resistance. Hence, the combination of both polymers offers an alternative to produce a low-cost material with good barrier properties. Since both polymers have a poor miscibility, a compatibilizer is commonly used in the formulations. Many works have been done about the compatibilization and the physical properties of these blends [1–5].

On the other hand, for materials to be used in structural or semi-structural applications, adequate fracture properties are also required. Commercial polypropylene homopolymer usually has the disadvantage of being quite brittle at room temperature and exhibiting poor resistance to crack propagation. However, the literature regarding the fracture properties of these blends is still limited [6–9] and, particularly these properties at extreme conditions such as impact loading and low temperatures have not been already investigated.

The main objective of this work was to study the deformation and fracture behavior of PP/EVOH blends compatibilized with ionomer Na<sup>+</sup> at room and low temperature. For this purpose, uniaxial tensile tests on dumb-bell samples and fracture tests on single-edge notched bending (SENB) specimens were performed for 10 wt.% and 20 wt.% EVOH blends with different ionomer content at 23 °C and –20 °C.

## 2. Experimental

### 2.1. Materials

An extrusion grade of poly(propylene) (PP) was synthesized by Repsol (ISPLEN PP044W3f). Its melt flow index (MFI) value is of 3.02 g/10 min (230 °C, 2160 g), and density 0.90 g cm<sup>-3</sup>.

The ethylene–vinyl alcohol copolymer (EVOH) from EVAL Europe (grade: F101B) has an ethylene content of 32.9%, a MFI of 1.51 g/10 min (190 °C, 2160 g), and density equal to 1.19 g cm<sup>-3</sup>.

In order to improve the miscibility between the PP and EVOH, it was necessary to add a compatibilizer to the blends. In this work, an ionomer Na<sup>+</sup> was used.

The ionomer Na<sup>+</sup> (Surlyn 8527) from Du Pont, is a random ethylene/methacrylic acid copolymer, in which the acid groups have been partially neutralized with sodium ions. The ionomer Na<sup>+</sup> have a MFI of 1.30 g/10 min (190 °C, 2160 g) and density equal to 0.94 g cm<sup>-3</sup>. It was expected that the ionomer Na<sup>+</sup> would interact by complexation with the OH groups of EVOH [3].

Melting points of the pure components and the blends determined by differential scanning calorimetry (DSC) and they were previously reported in Ref. [9].

### 2.2. Blends preparation

Prior to processing, EVOH and the ionomer Na<sup>+</sup> were dried in a vacuum oven for a period of 24 h at 80 °C and 8 h at 60 °C, respectively. Blends of PP/EVOH and PP/EVOH/ionomer Na<sup>+</sup> were prepared using a corotating twin-screw extruder (Brabender DSE20) operating at a speed of 45 rpm. The barrel temperature was 215 °C and the die temperature was 220 °C. All components were premixed by tumbling and simultaneously fed into the twin-screw extruder.

Binary blends were prepared in proportions 90/10 and 80/20, w/w PP/EVOH, respectively. The compatibilized blends were made with amounts of 2%, 5% and 10% of ionomer Na<sup>+</sup> respect the EVOH mass in the blend.

### 2.3. Sample preparation and mechanical characterization

Uniaxial tensile tests were carried out on Type Ia ISO 527-2:1993 dumb-bell specimens obtained by injection molding (Battenfeld Plus 350/75, 200 °C) in an INSTRON dynamometer 5566 at 10 mm/min, while break strength was determined at 20 mm/min, as some specimens did not reach its break point at 10 mm/min exceeding the dynamometer stroke.

In addition, pellets of the blends were compression-molded into thick plaques (thickness,  $B = 8$  mm) as explained elsewhere [9].

Fracture tests were performed in three-point bending on single-edge notched bend (SENB) specimens cut out from the compression-molded plaques in the INSTRON dynamometer at 1 mm/min by following ASTM D5045-93 recommendations [16].

In order to determine the effect of temperature on the blends behavior, fracture tests were carried out at room temperature and at –20 °C. The tests at low temperature were carried out into a climatic chamber with CO<sub>2</sub> ambient.

The resistance to crack initiation was characterized by the equivalent energy method originally proposed for Witt and Mager [10] to extend the applicability of the linear-elastic fracture mechanics (LEFM) to ductile metals. In this method, the equivalent energy parameter  $K_{IQ}^E$  is calculated from the maximum in the load–displacement curve as

$$K_{IQ}^E = \frac{F_{\max}^*}{B \cdot \sqrt{W}} \cdot f\left(\frac{a}{W}\right) \quad (1)$$

$$F_{\max}^* = \sqrt{2 \cdot U_{\max} \cdot \tan \alpha} \quad (2)$$

where  $B$ ,  $W$  and  $a$  are specimen thickness, depth and crack length, respectively,  $U_{\max}$  is the deformation energy at the maximum load and  $\tan \alpha$  is the initial slope of the load versus load–line displacement curve.

For SENB specimens:

$$f\left(\frac{a}{W}\right) = \frac{3 \cdot \frac{S}{W} \cdot \sqrt{\frac{a}{W}}}{2 \cdot \left(1 + 2 \cdot \frac{a}{W}\right) \cdot \left(1 - \frac{a}{W}\right)^{3/2}} \times \left[ 1.99 - \frac{a}{W} \left(1 - \frac{a}{W}\right) \left\{ 2.15 - 3.93 \left(\frac{a}{W}\right) + 2.7 \left(\frac{a}{W}\right)^2 \right\} \right] \quad (3)$$

#### 2.4. SEM fractography

The fracture surfaces of SENB specimens were examined using a JEOL JSM-6400 scanning electron microscope (SEM) at an accelerating voltage of 20 kV. The samples were sputter coated with a thin layer of gold before they were observed.

### 3. Results and discussion

#### 3.1. Fractographic analysis

Fracture surface observation for neat polypropylene at 23 °C was previously described [9] and it is presented in Fig. 1a for comparison. It revealed that some amount of stable crack (zone I) growth followed by unstable brittle fracture (zone II) existed in this material. On the other hand, the micrographs of Fig. 1b and c show the fracture surfaces of PP/EVOH blends with 10 wt.% and 20 wt.% EVOH, respectively obtained at room temperature. Differences between the stable crack propagation during the test (zone I) and the unstable fracture

promoted by high velocity and low temperature in a Charpy pendulum (zone II) to attain complete fracture of specimens as described elsewhere [9,11], are clearly observed in this figure. If the tests had not been interrupted, slow crack growth would have been extended through the whole ligament. The frontier area of zone I have a different appearance which can be assigned to a greater plastic deformation in the crack tip (see Fig. 1b and c).

Figs. 2 and 3 show microphotographs of the fast cryo-fractured surface region for the PP/EVOH blends with 10 wt.% and 20 wt.% EVOH, respectively.

The morphology of the blends is composed by the PP matrix containing elongated EVOH particles (dispersed phase) greater in the 20 wt.% than in the 10 wt.% EVOH blends (compare Fig. 2a with Fig. 3a). Figs. 2a and 3a and b showed typical brittle fracture surfaces where many EVOH particles are debonding of the PP matrix suggesting poor interfacial adhesion between both phases [4,5]. Therefore, during the crack propagation the fracture front preferentially passed from the particle–matrix interface rather than going through the particles. In addition, the increase in the ionomer  $\text{Na}^+$  content reduced the size of the dispersed phase confirming the compatibilizing effect of the ionomer  $\text{Na}^+$ .

Otherwise fracture surface observation for specimens tested at  $-20$  °C (Fig. 4) revealed that some amount of stable crack (zone I) growth followed by unstable fracture (zone II) existed in all materials. Therefore, the blends had more brittle behavior at low temperature than at room temperature, as was expected.

#### 3.2. Deformation behavior

Fig. 5 shows typical stress–strain curves obtained at 23 °C for pure components as well as for the blends with

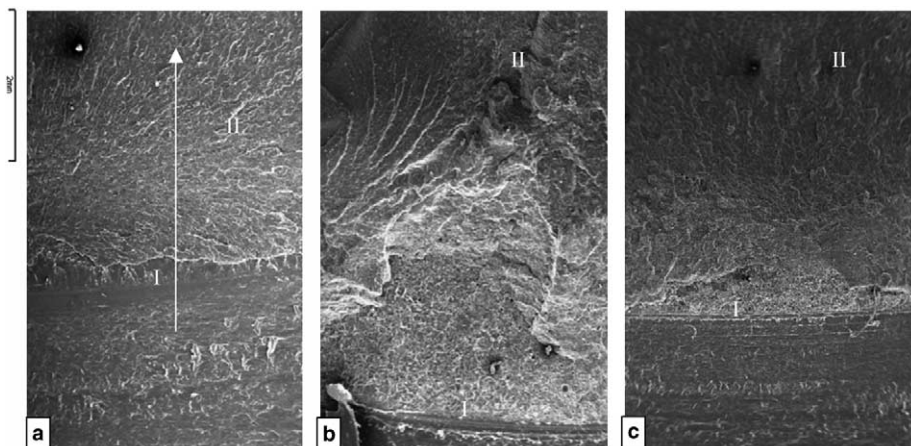


Fig. 1. Microphotographs of the fracture surface of PP/EVOH/ $\text{Na}^+$  samples tested at 23 °C showing two zones of crack propagation: I—stable, II—unstable. (a) PP, (b) 90/10/0 and (c) 80/20/0 (the arrow marks show the direction of crack propagation).

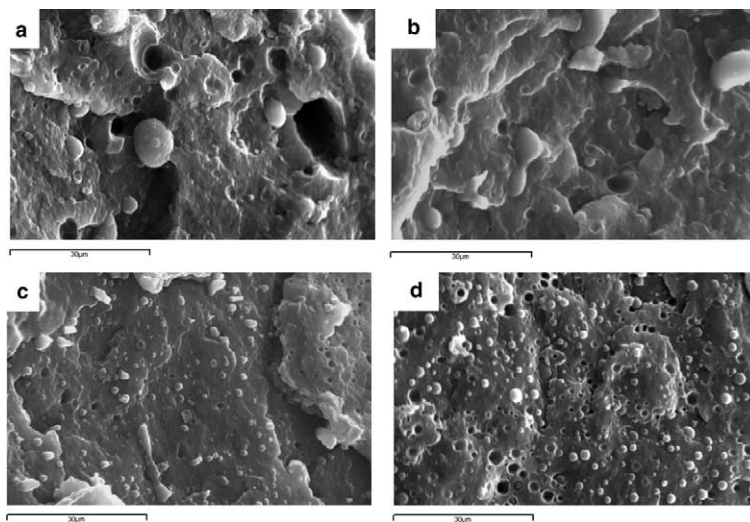


Fig. 2. Microphotographs of the fast cryo-fractured surface region for the 90/10 PP/EVOH blends: (a) 90/10/0, (b) 90/10/2, (c) 90/10/5, and (d) 90/10/10.

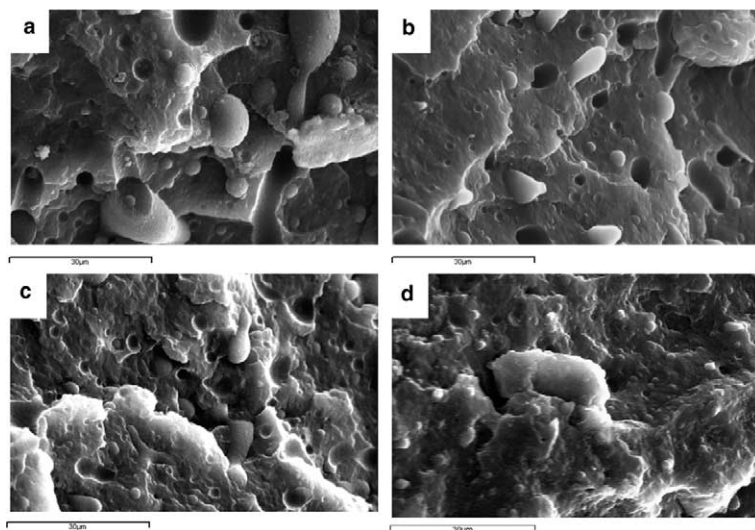


Fig. 3. Microphotographs of the fast cryo-fractured surface region for the 80/20 PP/EVOH blends: (a) 80/20/0, (b) 80/20/2, (c) 80/20/5, and (d) 80/20/10.

10 wt.% and 20 wt.% of EVOH without compatibilizer. The profile of the stress–strain curves for the samples with ionomer  $\text{Na}^+$  was similar. All PP samples displayed ductile behavior characterized by a decrease of load after yield (strain softening) followed by a plateau. All blends displayed less ductility than pure PP as a result of the poor interfacial adhesion between both phases and the subsequent particle debonding. The reduction in the failure strain was more significant in the samples with 20 wt.% of EVOH. Moreover, failure was observed almost immediately after maximum load in these blends.

It is also interesting to note that while PP samples developed a well defined stress whitened neck which stabilized and fractured with many shear band, in the PP/EVOH blends specimens, the neck was unable to stabilize and continued to thin down until failure.

Young's modulus, yield strength, deformation at yield, break strength and deformation at break were determined and the data obtained are presented in Table 1.

As it can be observed in Table 1, Young's modulus increases with the EVOH content as expected because EVOH elastic modulus is significantly higher than that

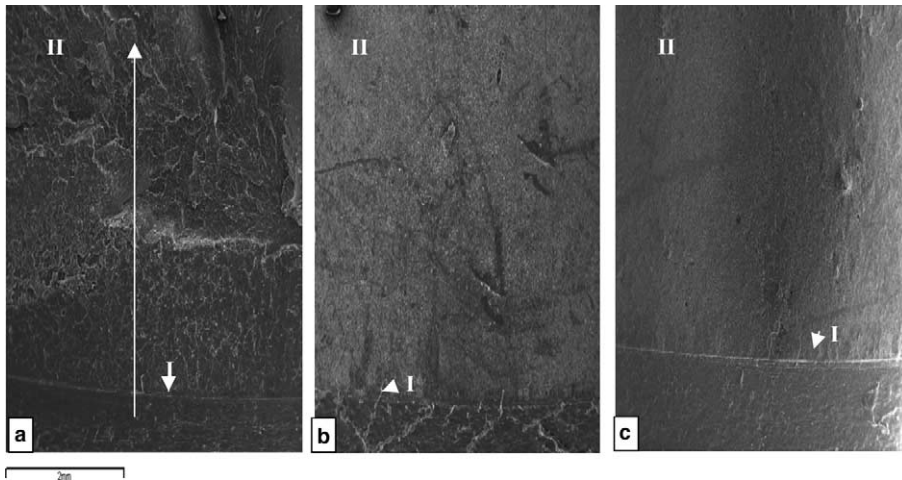


Fig. 4. Microphotographs of the fracture surface of PP/EVOH/Na<sup>+</sup> samples tested at  $-20^{\circ}\text{C}$  showing two zones of crack propagation: I—stable, and II—unstable. (a) PP, (b) 90/10/0 and (c) 80/20/0 (the arrow marks show the direction of crack propagation).

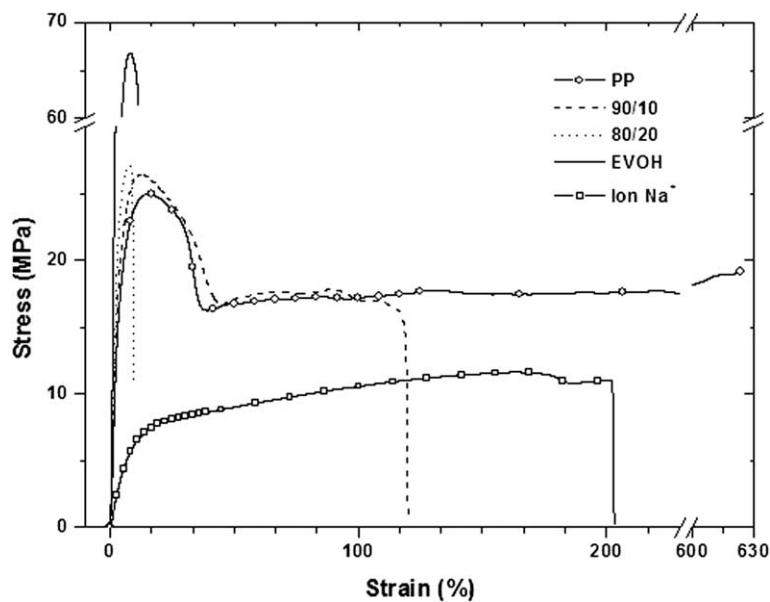


Fig. 5. Strain–stress curves for pure components and for the blends without compatibilizer.

of PP. In contrast, a decreasing trend of Young's modulus with ionomer content was found probably due to the low modulus of the ionomer Na<sup>+</sup> [12]. However, irrespectively of the ionomer content all blends still exhibited higher stiffness than pure PP. Also a decreasing trend of deformation at yield with EVOH content was observed. In addition, no significant differences in yield strength values with EVOH content or with the ionomer Na<sup>+</sup> content for each EVOH composition were found.

For the tensile properties at break point, incorporation of EVOH to PP drastically reduced deformation at break specially for the highest EVOH content investigated as pointed out above. It has been established in the literature [13], that low failure strain might be caused by particle debonding from the matrix prior to yielding as a result of poor interfacial adhesion. On the other hand, the ionomer Na<sup>+</sup> produced an improvement in the ductility of the blends. In general, the ionomer addition allowed an enhancement in the strain at the break point

Table 1  
Mechanical properties obtained at 23 °C with different test rate

Material	Young's modulus <sup>a</sup> (GPa)	Yield strength <sup>a</sup> (MPa)	Deformation at yield <sup>a</sup> (%)	Break strength <sup>b</sup> (MPa)	Deformation at break <sup>b</sup> (%)
PP	1.39 ± 0.11	24.73 ± 0.31	10.99 ± 0.46	21.74 ± 0.77	619.20 ± 4.70
90/10/0	1.60 ± 0.15	27.07 ± 0.55	8.34 ± 0.40	13.80 ± 1.83	113.80 ± 5.07
90/10/2	1.84 ± 0.29	27.19 ± 0.53	8.01 ± 0.45	10.63 ± 0.58	60.25 ± 13.90
90/10/5	1.62 ± 0.10	25.75 ± 0.82	8.29 ± 0.52	12.55 ± 1.99	92.58 ± 19.36
90/10/10	1.46 ± 0.11	25.71 ± 0.28	8.26 ± 0.18	9.62 ± 0.48	282.00 ± 33.77
80/20/0	1.85 ± 0.07	27.13 ± 0.55	5.48 ± 0.61	29.26 ± 0.68	8.50 ± 0.40
80/20/2	1.82 ± 0.09	27.10 ± 0.37	5.98 ± 0.19	29.17 ± 0.62	8.82 ± 0.17
80/20/5	2.08 ± 0.37	27.52 ± 0.50	6.54 ± 0.28	11.88 ± 1.87	34.25 ± 5.92
80/20/10	1.58 ± 0.19	27.88 ± 0.29	6.68 ± 0.59	12.92 ± 1.49	27.42 ± 5.63
EVOH	5.03 ± 0.83	67.80 ± 0.77	5.09 ± 0.14	28.26 ± 2.02	20.69 ± 2.45
Ionomer Na <sup>+</sup>	(30.33 ± 0.08) × 10 <sup>-3</sup>	11.66 ± 0.11	154.70 ± 0.86	11.50 ± 1.11	174.40 ± 5.95

<sup>a</sup> 10 mm/min.

<sup>b</sup> 20 mm/min.

and a more ductile fracture was observed in the ternary blends in comparison with the binary blends. The data obtained in other previous works [4,5], proved that the addition of ionomer produces an effective compatibilization in the 90/10 and 80/20 w/w PP/EVOH blends.

### 3.3. Fracture behavior

Fig. 6 shows load versus displacement traces recorded at 23 °C for SENB specimens of neat polypropylene and the blends with 10 wt.% and 20 wt.% EVOH.

Neat polypropylene exhibited nonlinear load–displacement behavior with some amount of slow crack growth preceding unstable fracture in agreement with

the results reported in literature for polypropylene homopolymer [14]. At initial steps stable crack propagation was observed and at a certain point in the load–displacement curve, the propagation mode suddenly changed. Crack propagation became unstable and samples separated into two halves [15]. This behavior can be referred to as semi-brittle.

On the contrary, all PP/EVOH blends displayed nonlinear load–displacement behavior with apparently stable crack growth (Fig. 6) and with no signs of sudden instability. Furthermore, fracture surfaces and side-views of broken specimens were stress whitened. Nevertheless, in several specimens the crack was observed to continue propagating even after the test had been inter-

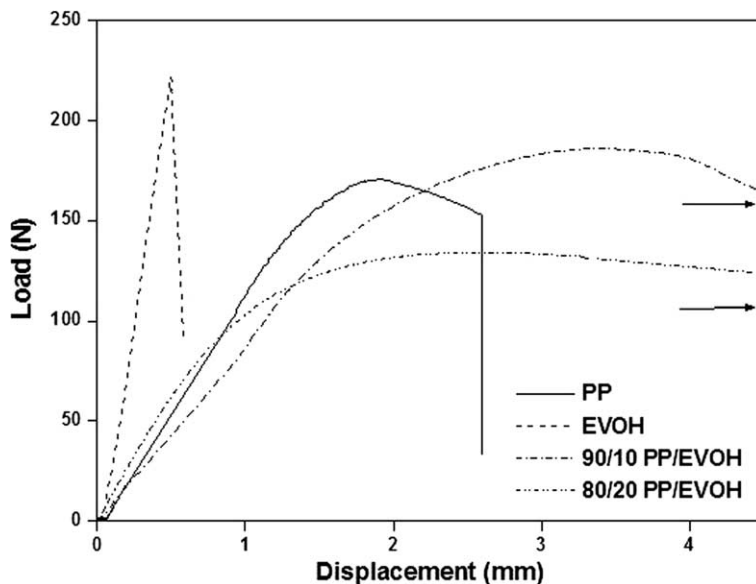


Fig. 6. Load versus displacement curves of SENB samples tested at 23 °C.

rupted without the need of additional energy. This behavior has been previously reported for PP/EVOH/ $Zn^{2+}$  blends [9] and referred to as “pseudo stable” behavior. It is also important to note that all blends displayed more ductile fracture behavior than PP as reflected from the significantly higher crack propagation displacement levels (post maximum range).

According to linear-elastic fracture mechanics [16], for valid plane strain fracture toughness determinations linear-elastic behavior up to the point of fracture and plane strain conditions are simultaneously needed [17–19]. Because these requirements were not satisfied in our experiments, energy equivalent parameter  $K_{I0}^E$  values were calculated and they were adopted here to compare the fracture initiation behavior of all materials. The results are shown in Fig. 7. Both PP/EVOH binary blends displayed lower values of resistance to crack initiation than pure polypropylene, probably due to the presence of critical-size flaws derived from debonding of second-phase particles that induced premature failure [13].

For all EVOH blends,  $K_{I0}^E$  increases with addition of 2 wt.% of ionomer  $Na^+$ , and it roughly remained constant with further addition of compatibilizer. As it was showed in the morphological analysis section, 10 wt.% EVOH blends exhibited smaller second-phase particles and also the incorporation of ionomer  $Na^+$  led to a decrease in the EVOH particle size for both 10 wt.% and 20 wt.% EVOH blends. The formation of critical-size flaws able to induce premature failure is likely to be suppressed as the particle size decreases [13]. Therefore, the better fracture resistance to crack initiation displayed by

10 wt.% EVOH blends can be attributed to a decrease in the critical-size flaw formation in smaller EVOH particles. However, the decrease in the EVOH particle size with the increase in ionomer  $Na^+$  content (upper 2%) was not enough to induce a further improvement in the fracture initiation parameter resistance in our blends.

Fig. 8 shows load versus displacement traces recorded at  $-20\text{ }^\circ\text{C}$  for SENB specimens of neat polypropylene and the blends with 10 wt.% and 20 wt.% EVOH.

At this low temperature, all materials exhibited non-linear load–displacement behavior with some amount of slow crack growth preceding unstable fracture and no additional energy was needed for further fracture crack propagation. In addition, in the blend specimens crack speed was lower than in neat PP samples and some hinging was also observed. Displacement level after maximum load which is a measure of ductile crack propagation was consequently higher for the blends.

Fig. 9 shows  $K_{I0}^E$  versus ionomer  $Na^+$  content determined at  $-20\text{ }^\circ\text{C}$  for neat polypropylene and the blends with 10 wt.% and 20 wt.% EVOH. It can also be observed that the values obtained at low temperature were slightly lower than those determined at  $23\text{ }^\circ\text{C}$ . In agreement with room temperature results, it can be observed that the addition of EVOH to PP was adverse to the resistance to crack initiation and that the addition of ionomer  $Na^+$  improved  $K_{I0}^E$  being this parameter roughly independent of ionomer content.

The results obtained here for the fracture behavior of PP/EVOH/ $Na^+$  blends at the two different temperatures investigated, can be explained in terms of the

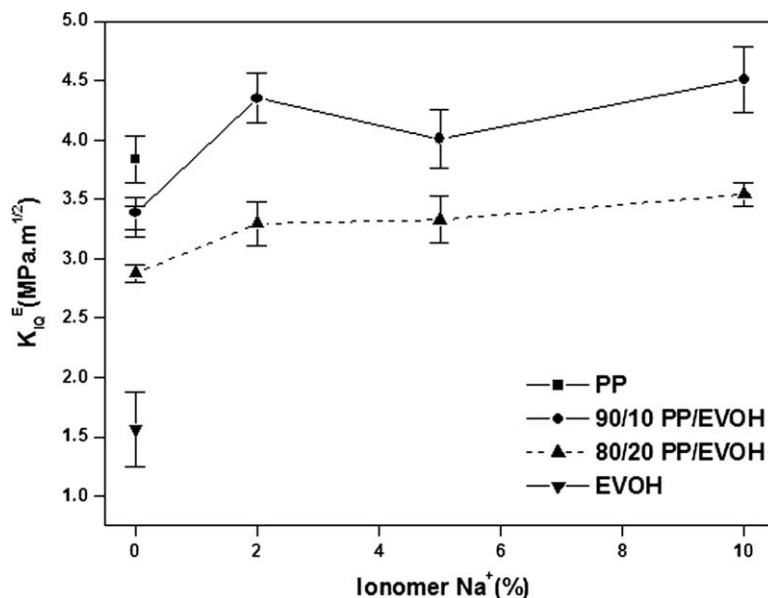


Fig. 7.  $K_{I0}^E$  versus ionomer content at  $23\text{ }^\circ\text{C}$ .

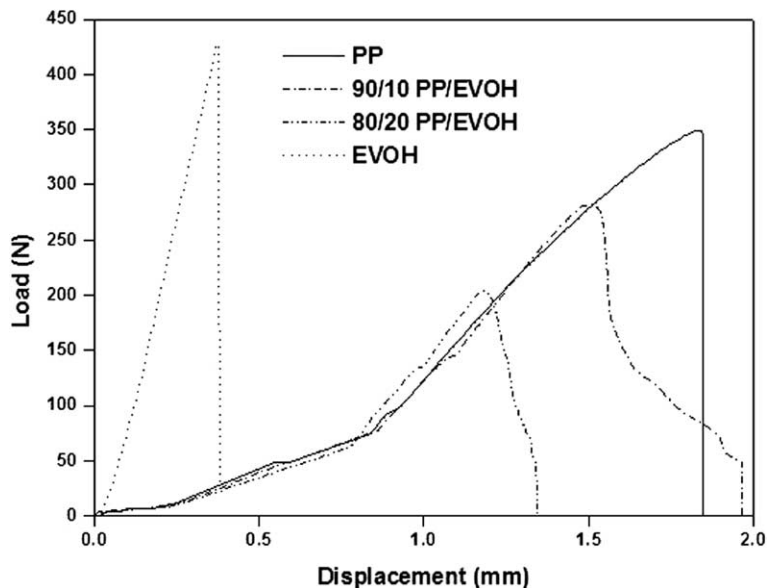


Fig. 8. Load versus displacement curves of SENB samples tested at  $-20\text{ }^{\circ}\text{C}$ .

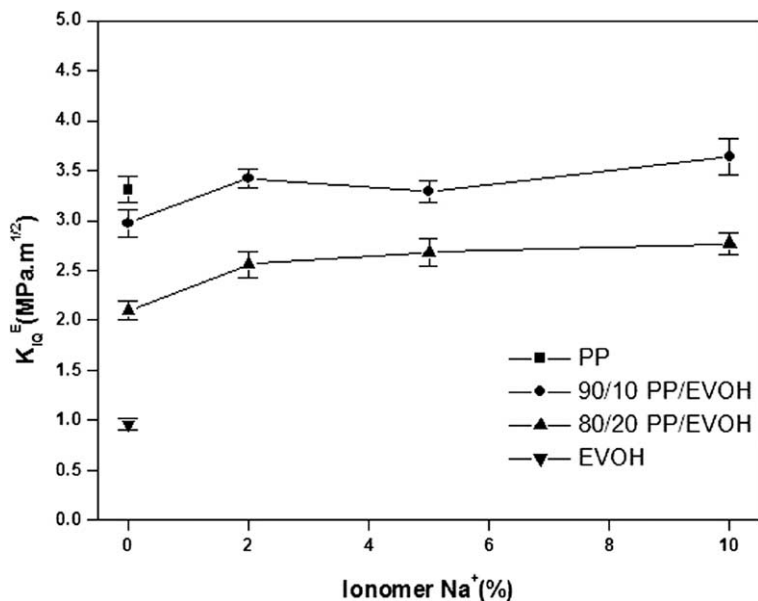


Fig. 9.  $K_{I0}^E$  versus ionomer content at  $-20\text{ }^{\circ}\text{C}$ .

brittle–ductile transition that many engineering materials exhibit with temperature [20–23]. At the brittle–ductile transition temperature (BDTT) the unstable crack propagation of a notched specimen characterized by a very high fracture speed becomes stable with a much lower fracture speed [22]. Otherwise, at low-test speeds this transition is a gradual process [21] which occurs

over a temperature range rather than at a single critical temperature. Therefore, the greater trend to stable crack propagation and the higher toughness values exhibited by the blends at  $23\text{ }^{\circ}\text{C}$  in comparison with those at  $-20\text{ }^{\circ}\text{C}$  could be attributed to the fact that the blends would be in the transition temperature range at these temperatures.



#### 4. Conclusions

In this work the deformation and fracture behavior of PP/EVOH blends compatibilized with ionomer Na<sup>+</sup> at room and below room temperature was investigated.

The incorporation of EVOH to PP led to less ductile materials in tension as judged by the lower values of the ultimate tensile strain displayed by all PP/EVOH blends in comparison to neat PP. In contrast, the ionomer Na<sup>+</sup> addition partially counteracted this detrimental effect.

The compatibilizing effect of ionomer Na<sup>+</sup> was also evident in fracture results since higher values of the fracture parameter were obtained for the blends with ionomer Na<sup>+</sup>. However, the increase in ionomer Na<sup>+</sup> content did not lead to further improvement in the resistance to fracture initiation. Therefore, a small amount of compatibilizer was enough to give the maximum attainable fracture parameter value without a significant loss of stiffness.

SEM observations also confirmed the compatibilizing effect of ionomer Na<sup>+</sup>.

On the other hand, PP/EVOH blends exhibited different fracture behavior with test temperature. All blends showed “pseudo stable” behavior at room temperature characterized by apparently stable crack growth that could not be externally controlled.

On the contrary, they behaved as semi-brittle at –20 °C with some amount of stable crack growth preceding unstable brittle fracture.

Finally, irrespectively of the temperature or the ionomer content all PP/EVOH blends always exhibited more ductile fracture behavior with a higher trend to stable crack propagation in comparison to neat polypropylene. This trend has been previously reported for similar blends and it has been explained in terms of the microscopic damage induced by debonding at the matrix/filler interface [9].

#### Acknowledgement

Financial support for this work has been provided by Secretaría Xeral de Investigación e Desenvolvemento, Xunta de Galicia through grant XUGA-PGIDT02TMT17201PR.

#### References

- [1] Faisant JB, Ait-Kadi A, Bousmina M, Deschenes L. *Polymer* 1998;39:533–45.
- [2] Demarquette NR, Kamal MR. *J Appl Polym Sci* 1998;70:75–87.
- [3] Kalfoglou NK, Samios CK, Papadopoulou CP. *J Appl Polym Sci* 1998;68:589–96.
- [4] Abad MJ, Ares A, Barral L, Cano J, Díez FJ, García-Garabal S, et al. *J Appl Polym Sci* 2004;94:1763–70.
- [5] Abad MJ, Barral L, Eguiazabal JI. *Polym Int* 2005;54:673–8.
- [6] Mai Y-W, Wong S-C, Chen X-H. In: Paul DR, Bucknall CB, editors. *Polymer blends*, vol. 2. New York: John Wiley & Sons; 2000. p. 17–58.
- [7] Grellmann W, Che M. *J Appl Polym Sci* 1997;66:1237–49.
- [8] Niebergall U, Bohse J, Seidler S, Grellmann W, Schürmann BL. *Polym Eng Sci* 1999;39:1109–18.
- [9] Montoya M, Abad MJ, Barral L, Bernal C. *J Appl Polym Sci*, in press.
- [10] Witt F, Mager TR. *Nucl Des* 1971;17:91–102.
- [11] Gensler R, Plummer CJG, Grein C, Kausch H-H. *Polymer* 2000;41:3809–19.
- [12] Kim Y, Ha C-S, Kang T-K, Kim Y, Cho W-J. *J Appl Polym Sci* 1994;51:1453–61.
- [13] Wong S-C, Mai Y-W. *Polymer* 1999;40:1553–66.
- [14] Frontini PM, Fave A. *J Mater Sci* 1995;30:2446–54.
- [15] Santarelli E, Frontini P. *Polym Eng Sci* 2001;41:1803–14.
- [16] Standard test methods for plane-strain fracture toughness and energy release rate determination of plastics materials, ASTM D 5045-93. American Society for Testing and Materials, 1993.
- [17] Che M, Grellmann W, Seidler S, Landes JD. *Fatigue Fract Eng Mater Struct* 1997;20:119–27.
- [18] Morhain C, Velasco JI. *J Mater Sci* 2001;36:1487–99.
- [19] Lu M, Chiou K-C, Chang F-C. *Polym Eng Sci* 1996;36:2289–95.
- [20] Kinloch AJ, Young RJ. *Fracture behaviour of polymers*. London: Applied Science Publishers Ltd; 1983.
- [21] van der Wals A, Nijhof R, Gaymans RJ. *Polymer* 1999;40:6031–44.
- [22] van der Wals A, Verheul AJJ, Gaymans RJ. *Polymer* 1999;40:6057–65.
- [23] Zebarjad SM, Lazzeri A, Bagheri R, Seyed Reihani SM, Frounchi M. *Mater Lett* 2003;57:2733–41.